

Electronic Supplementary Information for

Two novel 3-D coordination polymers with 5-methoxyisophthalate and flexible N-donor co-ligands showing pentanuclear or alternate mono/binuclear Cu(II) units

Lu-Fang Ma,^a Jun-Wei Zhao,^b Min-Le Han,^a Li-Ya Wang^{a*} and Miao Du^{c*}

^a College of Chemistry and Chemical Engineering, Luoyang Normal University, Luoyang 471022, China; ^b College of Chemistry and Chemical Engineering, Henan University, Kaifeng 475001, China; ^c College of Chemistry, Tianjin Key Laboratory of Structure and Performance for Functional Molecule, Tianjin Normal University, Tianjin 300387, China

To whom correspondence should be addressed.

E-mail address: wlya@lynu.edu.cn (L.-Y. Wang), Tel./Fax: +86-379-65511205

dumiao@public.tpt.tj.cn (M. Du), Tel./Fax: +86-22-23766556

Table S1. Selected bond lengths (Å) and angles (°) for **1** and **2**^a.

1			
Cu(1)–O(11)	1.9452(17)	O(11)–Cu(1)–O(3)#2	83.92(7)
Cu(1)–O(11)#1	1.9452(17)	O(11)#1–Cu(1)–O(3)#2	96.08(7)
Cu(1)–O(2)#1	1.9956(18)	O(2)#1–Cu(1)–O(3)#2	89.89(8)
Cu(1)–O(2)	1.9956(19)	O(2)–Cu(1)–O(3)#2	90.11(8)
Cu(1)–O(3)#2	2.4054(19)	O(11)–Cu(1)–O(3)#3	96.08(7)
Cu(1)–O(3)#3	2.4054(19)	O(11)#1–Cu(1)–O(3)#3	83.92(7)
Cu(2)–O(4)#3	1.9417(19)	O(2)#1–Cu(1)–O(3)#3	90.11(8)
Cu(2)–O(9)#4	1.948(2)	O(2)–Cu(1)–O(3)#3	89.89(8)
Cu(2)–O(11)	1.9497(18)	O(3)#2–Cu(1)–O(3)#3	180.00(6)
Cu(2)–N(1)	1.993(3)	O(4)#3–Cu(2)–O(9)#4	156.86(9)
Cu(3)–O(6)	1.944(2)	O(4)#3–Cu(2)–O(11)	99.54(8)
Cu(3)–O(11)	1.9652(17)	O(9)#4–Cu(2)–O(11)	88.55(8)
Cu(3)–O(1)	1.9668(19)	O(4)#3–Cu(2)–N(1)	95.18(10)
Cu(3)–N(3)	1.991(2)	O(9)#4–Cu(2)–N(1)	92.42(10)

O(11)–Cu(1)–O(11)#1	180.00(7)	O(11)–Cu(2)–N(1)	139.56(10)
O(11)–Cu(1)–O(2)#1	88.63(8)	O(6)–Cu(3)–O(11)	93.69(8)
O(11)#1–Cu(1)–O(2)#1	91.37(8)	O(6)–Cu(3)–O(1)	171.74(9)
O(11)–Cu(1)–O(2)	91.37(8)	O(11)–Cu(3)–O(1)	94.56(8)
O(11)#1–Cu(1)–O(2)	88.63(8)	O(6)–Cu(3)–N(3)	86.14(10)
O(2)#1–Cu(1)–O(2)	180.0	O(11)–Cu(3)–N(3)	179.18(10)
2			
Cu(1)–O(2)#1	1.975(3)	O(1)–Cu(1)–N(1)	97.14(12)
Cu(1)–O(1)	1.980(2)	O(7)#1–Cu(1)–N(1)	95.40(11)
Cu(1)–O(7)#1	1.980(3)	O(6)–Cu(1)–N(1)	96.42(11)
Cu(1)–O(6)	1.993(2)	O(2)#1–Cu(1)–Cu(1)#1	81.54(8)
Cu(1)–N(1)	2.131(3)	O(1)–Cu(1)–Cu(1)#1	86.60(7)
Cu(1)–Cu(1)#1	2.6456(8)	O(7)#1–Cu(1)–Cu(1)#1	85.31(8)
Cu(2)–O(4)	1.970(2)	O(6)–Cu(1)–Cu(1)#1	82.86(7)
Cu(2)–O(4)#2	1.970(2)	N(1)–Cu(1)–Cu(1)#1	176.20(9)
Cu(2)–N(6)#3	1.972(3)	O(4)–Cu(2)–O(4)#2	180.0
Cu(2)–N(6)#4	1.972(3)	O(4)–Cu(2)–N(6)#3	90.05(12)
Cu(3)–O(11)	1.930(3)	O(4)#2–Cu(2)–N(6)#3	89.95(12)
Cu(3)–O(11)#5	1.930(3)	O(4)–Cu(2)–N(6)#4	89.95(12)
Cu(3)–O(9)	1.931(3)	O(4)#2–Cu(2)–N(6)#4	90.05(12)
Cu(3)–O(9)#5	1.931(3)	N(6)#3–Cu(2)–N(6)#4	180.000(1)
O(2)#1–Cu(1)–O(1)	168.07(10)	O(11)–Cu(3)–O(11)#5	180.00(17)
O(2)#1–Cu(1)–O(7)#1	89.03(12)	O(11)–Cu(3)–O(9)	91.79(12)
O(1)–Cu(1)–O(7)#1	88.72(11)	O(11)#5–Cu(3)–O(9)	88.21(12)
O(2)#1–Cu(1)–O(6)	89.46(11)	O(11)–Cu(3)–O(9)#5	88.21(12)
O(1)–Cu(1)–O(6)	90.35(11)	O(11)#5–Cu(3)–O(9)#5	91.79(12)
O(7)#1–Cu(1)–O(6)	168.17(10)	O(9)–Cu(3)–O(9)#5	180.000(1)

^aSymmetry codes: **1**: #1 $-x+1, -y+2, -z$; #2 $-x+3/2, y+1/2, -z+1/2$; #3 $x-1/2, -y+3/2, z-1/2$; #4 $-x+1/2, y-1/2, -z+1/2$, **2**: #1 $-x+1, -y+1, -z+2$; #2 $-x, -y, -z+1$; #3 $-x, -y, -z+2$; #4 $x, y, z-1$; #5 $-x+1, -y+2, -z+1$.

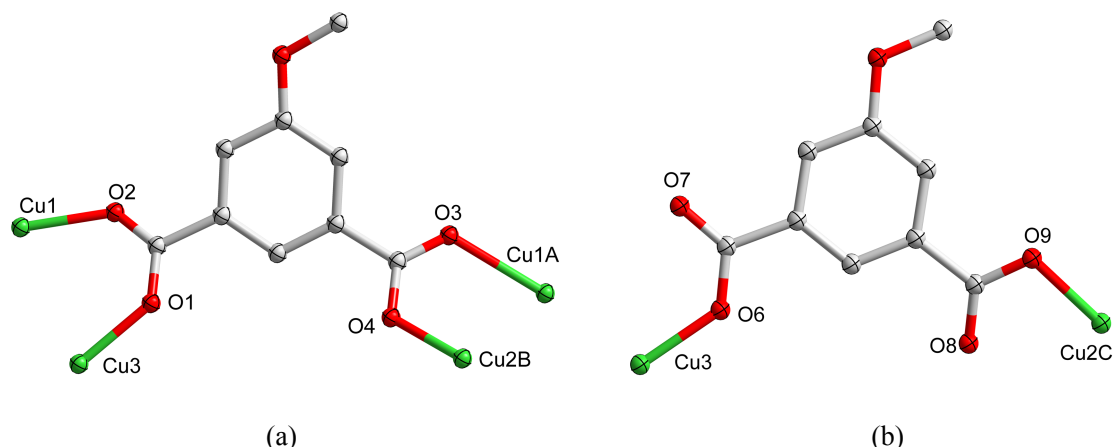


Fig. S1. Coordination modes of $\text{CH}_3\text{O-ip}$ ligands in **1** (symmetry codes: A: $-x + 3/2, y - 1/2, -z + 1/2$; B: $x + 1/2, -y + 3/2, z + 1/2$; C: $-x + 1/2, y + 1/2, -z + 1/2$).

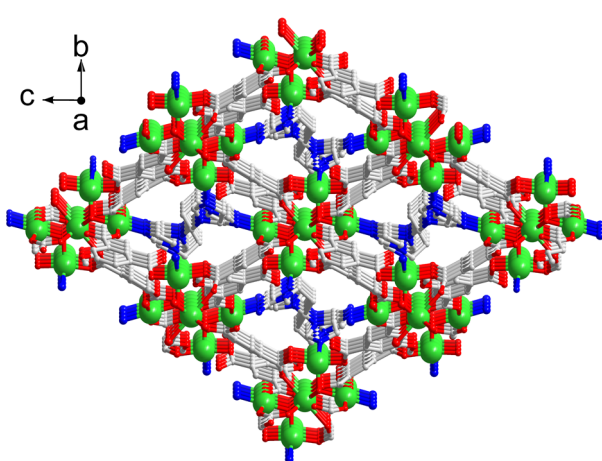


Fig. S2. Ball and stick view of the overall 3-D network of **1**.

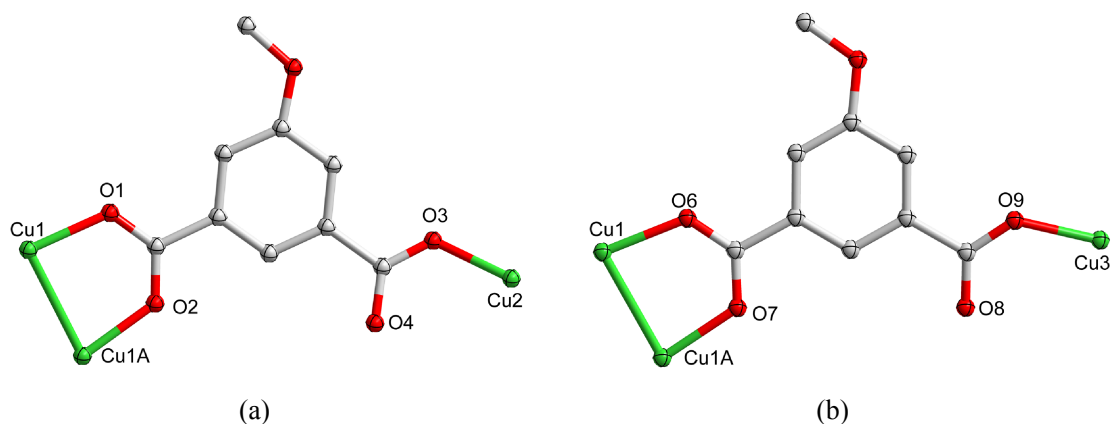


Fig. S3. Coordination modes of $\text{CH}_3\text{O-ip}$ ligands in **2** (symmetry code: A: $-x + 1, y + 1, -z + 2$).

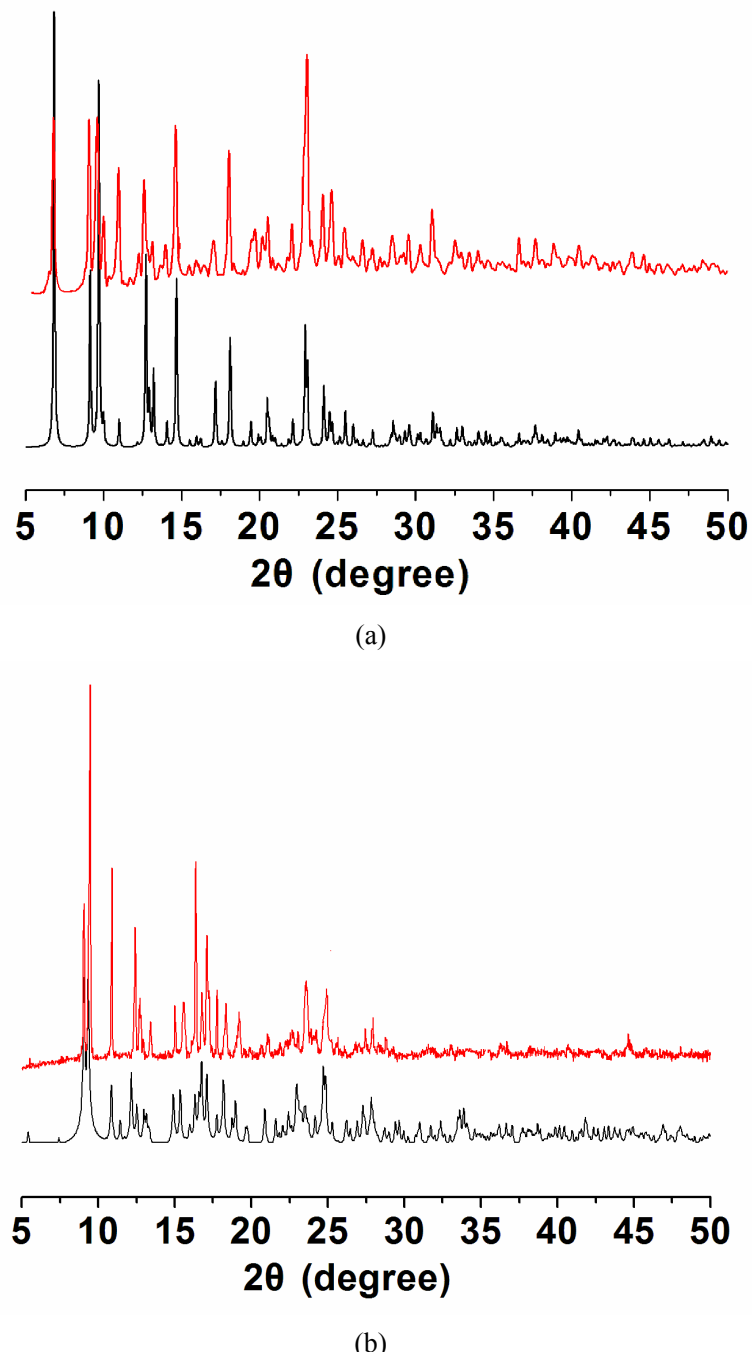
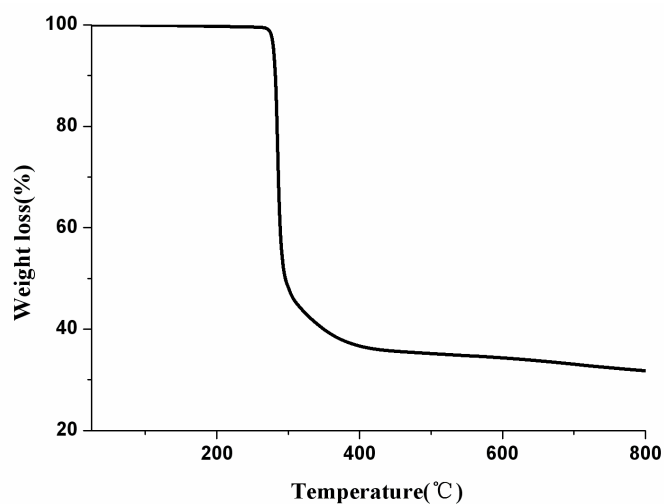
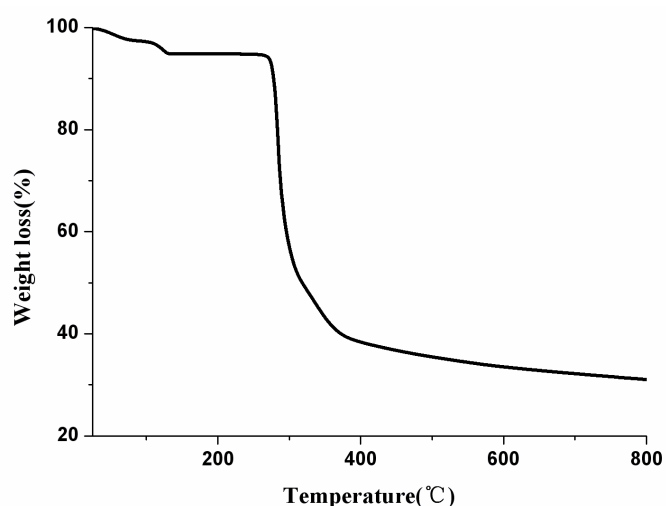


Fig. S4. Simulated (black) and experimental (red) XRPD patterns of (a) **1** and (b) **2**.



(a)

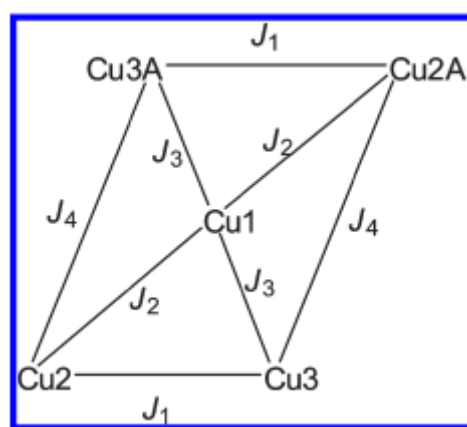


(b)

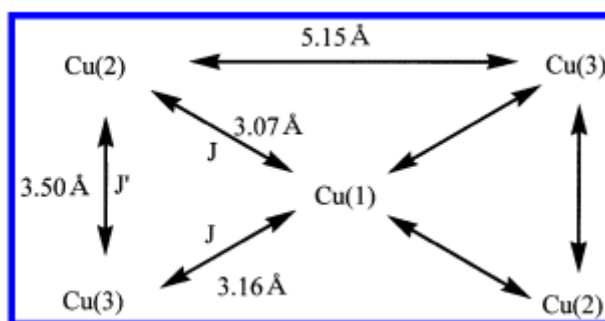
Fig. S5. TG curves of (a) **1** and (b) **2**.

The details for magnetic pathways and interactions in $\{[\text{Cu}_5(\text{bime})(\mu_3\text{-OH})_2(\text{phth})_4](\text{H}_2\text{O})_2\}_n$ (bime = 1,2-bis(imidazol-1-yl)ethane, phth = 1,2-benzenedicarboxylate): The observed J values can be correlated to the molecular structure by considering the available exchange pathways between the Cu(II) ions. Cu1…Cu3 and Cu2…Cu3 are connected via a $\mu_3\text{-OH}$ bridge with the bridging angles 97.02(9) and 101.37(9) $^\circ$, respectively, and therefore show ferromagnetic interactions ($J_3 = 48.33 \text{ cm}^{-1}$, $J_1 = 16.67 \text{ cm}^{-1}$). On the other hand, Cu1…Cu2 is linked by a $\mu_3\text{-OH}$ bridge with the bridging angle of 128.26(11) $^\circ$, which results in an antiferromagnetic exchange interaction ($J_2 = -17.43 \text{ cm}^{-1}$). Cu2…Cu3A is joined by one O2-C-O1 carboxylate group and shows a weak ferromagnetic interaction ($J_4 = 7.90 \text{ cm}^{-1}$). The interpentamer magnetic exchange interaction through the phth bridges shows a very weak ferromagnetic interaction ($J' = 0.040 \text{ cm}^{-1}$).

Exchange pathways in $\{[\text{Cu}_5(\text{bime})(\mu_3\text{-OH})_2(\text{phth})_4](\text{H}_2\text{O})_2\}_n$



The details for magnetic pathways and interactions in $\{[(\text{en})\text{Pt}(\text{nic})_2)_3\text{Cu}_5(\text{OH})_2(\text{OH}_2)_6\}(\text{NO}_3)_8\}_n$ (nic = nicotinate): The temperature-dependent curve of the magnetism of the crystal is fitted with an equation that describes the magnetism of such a trinuclear system best at $g = 2.22$, $J/k = -16 \text{ K}$, and $J'/k = 90 \text{ K}$. The fitted values imply that antiferromagnetic and ferromagnetic couplings coexist in the system.



The details for magnetic pathways and interactions in $[\text{Cu}_5(\text{O}_2\text{CMe})_6\{\text{pyC(O)(OH)pyC(O)(OH)py}\}_2]$ ($\text{pyCopyCopy} = 2,6\text{-di-(2-pyridylcarbonyl)-pyridine}$): The triply bridged $[\text{Cu}_2(\text{OR})_2(\text{O}_2\text{CMe})]^+$ moiety with unequal Cu–O–Cu angles and bent Cu_2O_2 core is rather complicated and will be treated qualitatively. First, we may suppose that the main superexchange pathway will be through O(3), which occupies the magnetic orbitals of both Cu(2) and Cu(3) (of $d_{x^2-y^2}$ character for both atoms). Conversely, O(14) which is situated at the apical positions of both square pyramids, is expected to contribute less to the magnetic exchange since it occupies nonmagnetic orbitals (of d_{z^2} character). In both cases the small Cu–O–Cu angles are not expected to favor the antiferromagnetic interactions. But most importantly, the small dihedral angle of the Cu_2O_2 core is expected to enhance the ferromagnetic character of the interaction by limiting the overlap of the magnetic orbitals of Cu(2) and Cu(3). On the other hand, the antiferromagnetic interaction J_2 is in agreement with the large Cu(2)–O(1)–Cu(1) angle (120.94°) in which the O(1) monoatomic bridge occupies the magnetic orbitals of both Cu(1) and Cu(2).

